

# Responding to Temperature Changes

## CHAPTER PREVIEW

Heat is essentially the vibration of atoms in a material. Consequently thermal properties reflect the type and strength of interatomic bonding and the crystal structure. The important thermal properties of any material are

- Heat capacity
- Coefficient of thermal expansion
- Thermal conductivity

Thermal properties of ceramics differ from those of metals whenever free (conduction) electrons are involved, such as in thermal conductivity. However, heat transfer by phonon (lattice vibration) transport can in some cases be more effective than through the movement of electrons. We describe melting and vaporization of ceramics as the temperatures for these transformations tend to be high, which can be critical in certain applications, such as the tiles on the space shuttle, but present problems during processing. It should also be obvious by now that heat affects many of the properties of ceramics such as Young's modulus, electrical conductivity, magnetic behavior, and dielectric constant. There are major applications that utilize the varied thermal properties of ceramics, from high thermal conductivity substrates for electronic packaging to enormous mirror blanks for telescopes that have "zero" expansion.

### 34.1 SUMMARY OF TERMS AND UNITS

Table 34.1 lists the important parameters used in this chapter and their units. The SI unit of temperature is kelvin (K), but as you will have realized by now °C is often used in presenting data in materials science. As mentioned in Chapter 1, the numerical value of a temperature difference or temperature interval expressed in °C is equal to the numerical value of the same temperature difference or interval when expressed in K. This point is worth remembering when coefficients of thermal expansion or thermal conductivities are compared for different materials.

### 34.2 ABSORPTION AND HEAT CAPACITY

When a solid absorbs an amount of heat,  $dq$ , its internal energy,  $E$ , rises by an amount  $dE$  where

$$dE = dq \quad (34.1)$$

The increase in internal energy is largely due to the increased vibrational amplitude of the atoms about their

equilibrium positions. This vibrational motion represents the thermal energy of the solid. There are other mechanisms for heat absorption, but these are either negligible or absent entirely. However, we will list them here and very briefly describe them because they relate to some concepts that have been described in earlier chapters such as point defects.

- *Rotational*: Rotational absorption is important in liquids and gases where the molecules are free to rotate, but this contribution is negligible in solids.
- *Electronic*: Absorption by conduction electrons is very small, but it can be used to provide information about the electronic structure of a solid, so from that point of view it is useful.
- *Defect formation*: The formation of Frenkel and Schottky defects can contribute, although usually only at high temperatures.
- *Phase transformations*: These involve absorption by structural, magnetic, and ferroelectric transformations in certain materials.

Heat capacity is a measure of the amount of energy required to raise the temperature of a material. At room

**TABLE 34.1 Summary of Terms Used to Describe the Thermal Properties of Materials**

	Definition	Units/value
$\alpha$	Linear coefficient of thermal expansion	$^{\circ}\text{C}^{-1}$ or $\text{K}^{-1}$
$C_v$	Heat capacity at constant volume	J/K
$c_v$	Molar heat capacity at constant volume	$\text{J mol}^{-1} \text{K}^{-1}$
$C_p$	Heat capacity at constant pressure	J/K
$c_p$	Molar heat capacity at constant pressure	$\text{J mol}^{-1} \text{K}^{-1}$
$\Delta S_f$	Entropy of fusion	$\text{J mol}^{-1} \text{K}^{-1}$ or $\text{J g-atom}^{-1} \text{K}^{-1}$
$\Delta S_v$	Entropy of vaporization	$\text{J mol}^{-1} \text{K}^{-1}$ or $\text{J g-atom}^{-1} \text{K}^{-1}$
$k$	Thermal conductivity	$\text{W m}^{-1} \text{K}^{-1}$
$T_b$	Boiling temperature	$^{\circ}\text{C}$ or $\text{K}$
$T_m$	Melting temperature	$^{\circ}\text{C}$ or $\text{K}$
$R_{\text{TS}}$	Thermal shock resistance	W/m
$\theta_D$	Debye temperature	$^{\circ}\text{C}$ or $\text{K}$
$R$	Gas constant	$8.314 \text{ J mol}^{-1} \text{K}^{-1}$

temperature the specific heat capacity of many ceramics is between 0.75 and  $1.0 \text{ J g}^{-1} \text{K}^{-1}$ . For example, granite (an igneous silicate rock) has a specific heat capacity of  $0.79 \text{ J g}^{-1} \text{K}^{-1}$  at  $25^{\circ}\text{C}$ , which means that it takes about 0.8 J of energy to raise the temperature of 1 g of granite by 1 K. Water has a specific heat capacity of  $4.184 \text{ J g}^{-1} \text{K}^{-1}$  at  $25^{\circ}\text{C}$ ; this value is more than five times greater than that of granite. This difference is crucial in regulating the earth's temperature. It takes five times more energy to increase the temperature of water by 1 K than it does to increase the temperature of granite. If the earth's surface were composed entirely of rock (i.e., there were no oceans) then daytime temperatures would be extremely high. The oceans also help limit the temperature drop at night, because they have absorbed more energy during the day, which is released at night. If the earth had no oceans temperature swings between day and night would be very large.

When referring to heat capacity, and in particular when various other sources are consulted, it is necessary to be careful about terminology. Here are the definitions of all the terms you are likely to encounter:

- Heat capacity is the amount of heat required to change the temperature of an object by 1 K. The units of heat capacity are J/K.
- Specific heat capacity is the amount of heat required to change the temperature of 1 g of a substance by 1 K. The units of specific heat capacity are  $\text{J g}^{-1} \text{K}^{-1}$ .
- Molar heat capacity is the amount of heat required to change the temperature of 1 mol of a substance by 1 K. The units of molar heat capacity are  $\text{J mol}^{-1} \text{K}^{-1}$ .

In the literature you will find that “heat capacity” is often used to describe all these three terms. But it is usually obvious from the units given what term is actually the correct one to use. The next term is really the confusing one. Fortunately it is not used now, but it does occur from time to time in some of the older literature so beware:

- Specific heat is the ratio of the heat capacity of a substance to the heat capacity of water. This term is a unitless ratio and was used when the heat capacity of water was unity. In the SI system of units the heat capacity of water is not unity.

Heat capacities of solids are always functions of temperature, as illustrated for several ceramics in Figure 34.1. Note the units are  $\text{J g-atom}^{-1} \text{K}^{-1}$ . At absolute zero the internal energy of a solid is a minimum and the heat capacity is zero. As the temperature rises the heat capacity increases, which is indicative of the various mechanisms by which energy is absorbed. The heat capacity approaches

a classical limit of  $3R$  ( $\sim 25 \text{ J mol}^{-1} \text{K}^{-1}$ ) at a sufficiently high temperature that differs from one solid to another. This statement is essentially the Dulong–

Petit law. The crystal structure and composition of a material do not appreciably affect heat capacity but  $n$  does: e.g.,  $c_p$  is  $3R$  for Cu but  $6R$  for MgO.

The temperature at which the heat capacity becomes constant, or varies only slightly with temperature, is the Debye temperature,  $\theta_D$ . Values of  $\theta$  are typically in the range of  $T_m/5$  to  $T_m/2$  and depend on

- Bond strength
- $E$
- $T_m$

For example, in diamond, where the covalent bonds are very strong,  $\theta_D$  is  $\sim 2000 \text{ K}$ . However, the value of  $\theta_D$  for NaCl is  $281 \text{ K}$ .

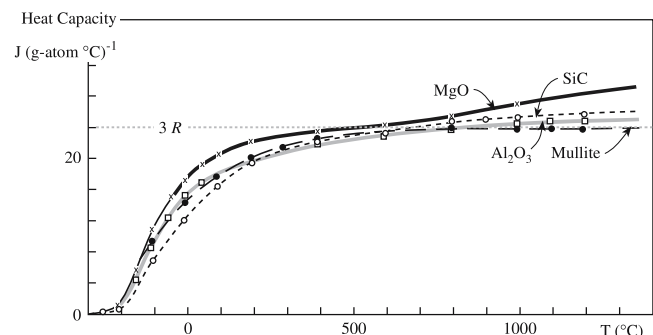


**FIGURE 34.1** Heat capacity of some ceramics as a function of temperature.

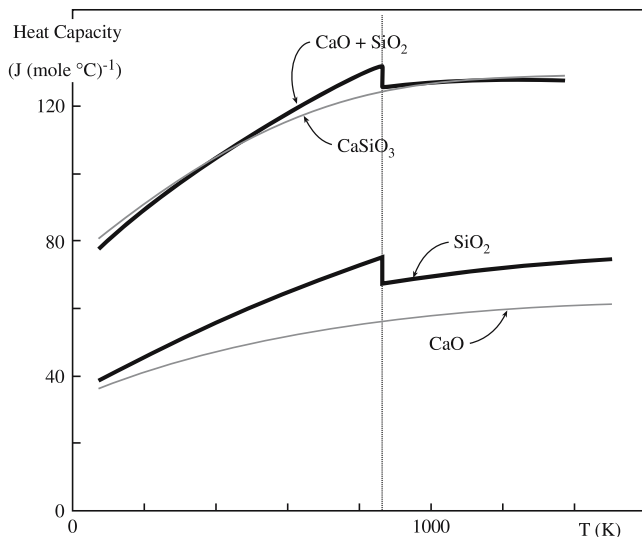


FIGURE 34.2 Heat capacity of SiO<sub>2</sub> as a function of temperature.

Abrupt changes in heat capacity are observed over a narrow temperature range when a material undergoes a structural transformation or some other change in order. The example shown in Figure 34.2 is for quartz (a polymorph of SiO<sub>2</sub>), which undergoes a displacive  $\alpha$ - $\beta$  phase transformation at 573°C. Similar changes in heat capacity occur in glasses at the glass transition temperature,  $T_g$ , because of the increase in configurational entropy in the liquid. Anomalous heat capacities are also associated with the alignment of magnetic dipoles in ferromagnetic materials and the alignment of electric dipoles in ferroelectrics.

The heat capacity of a material can be calculated, depending on the temperature range of interest, using one of two equations. At very low (cryogenic) temperatures

$$c_p \cong c_v = K \left( \frac{T}{\theta_D} \right)^3 + \gamma T \quad (34.2)$$

where  $K$  is a constant equal to  $1940 \text{ J mol}^{-1} \text{ K}^{-1}$  and  $\gamma$  is the electronic heat capacity coefficient. Values of  $\theta_D$  and  $\gamma$  are tabulated in several lists of thermodynamic properties. These values are generally widely available for metals and somewhat more obscure for most ceramics. The overall contribution of Eq. 34.2 to the heat capacity of a material is small and is really of importance only if you wish to obtain a fundamental understanding of the nature of a material or if you are designing systems to operate at cryogenic temperatures.

At high temperature (usually above room temperature) heat capacities can be calculated using the empirical relation

$$c_p = a + bT + cT^{-2} \text{ J mol}^{-1} \text{ K}^{-1} \quad (34.3)$$

where  $a$ ,  $b$ , and  $c$  are “constants,” which have been tabulated for a wide range of materials.

### 34.3 MELTING TEMPERATURES

One of the very useful properties of many ceramics is their high  $T_m$  as shown in Table 34.2. This property makes ceramics without equal for application at high temperature, such as refractories and thermal barrier coatings. There is a direct correlation between  $T_m$  and bond strengths. Also, ceramics with the highest values of  $T_m$  tend to have a significant fraction of covalent character to their bonding as shown in Table 34.3; this table is calculated using Eq. 4.24 and values of Pauling electronegativities given in Figure 3.4. However,  $T_m$  does not correlate directly with the fraction of covalent character of the bond or ionic potential ( $\phi$ ) of the cation as shown for the oxides of the alkaline earth elements in Table 34.4, which is calculated in the same manner. (The values of ionic radii are given in Table 4.6.)

Compounds with very high fractions of ionic character to their bonds such as the alkali halides NaCl and LiF tend to have lower values of  $T_m$  than their corresponding oxides. The reason is the greater ionic charges (e.g., O<sup>2-</sup> rather than Cl<sup>-</sup>) involved and hence the stronger electrostatic attraction. We can illustrate this point for the two compounds Li<sub>2</sub>O and LiF. Bond energies for ionic compounds can be obtained using Eq. 34.4 (this is simply the Born-Landé equation given in Chapter 4 written for a single bond):

$$E_{\text{bond}} = \frac{Z_1 Z_2 e^2}{4\pi\epsilon_0 r_0} \left( 1 - \frac{1}{n} \right) \quad (34.4)$$

For Li<sub>2</sub>O we have  $r_{\text{Li}^+} = 0.068 \text{ nm}$  and  $r_{\text{O}^{2-}} = 0.140 \text{ nm}$ , so  $r_0 = 0.208 \text{ nm}$ . Taking  $n = 10$ , and substituting into Eq. 34.4 we get a value of  $E_{\text{bond}} = 1.997 \times 10^{-18} \text{ J}$ .

For LiF we have  $r_{\text{Li}^+} = 0.068 \text{ nm}$  and  $r_{\text{F}^-} = 0.133 \text{ nm}$ , so  $r_0 = 0.201 \text{ nm}$ . Taking  $n = 10$  and substituting into Eq. 34.4 we get a value of  $E_{\text{bond}} = 1.033 \times 10^{-18} \text{ J}$ .

So we would expect Li<sub>2</sub>O to have a higher  $T_m$  than LiF, and if you look at Table 34.2 you will see that for Li<sub>2</sub>O  $T_m = 1570^\circ\text{C}$  while for LiF  $T_m = 848^\circ\text{C}$ .

The entropy difference between the solid and the liquid at  $T_m$  is

$$\Delta S_f = \frac{\Delta H_f}{T_m} \quad (34.5)$$

#### RICHARD'S RULE

$$\Delta S_f = 8.4 \text{ J g-atom}^{-1} \text{ K}^{-1}$$

Values of  $\Delta S_f$  are shown in Table 34.2. They are positive because the liquid is

always more disordered than the solid, but vary considerably from the empirical prediction known as Richard's

**TABLE 34.2  $T_m$  and  $\Delta S_f$  for Selected Ceramics**

Compound	$T_m$ ( $^{\circ}\text{C}$ )	$\Delta S_f$ ( $\text{J mol}^{-1} \text{ }^{\circ}\text{C}^{-1}$ )	Compound	$T_m$ ( $^{\circ}\text{C}$ )	$\Delta S_f$ ( $\text{J mol}^{-1} \text{ }^{\circ}\text{C}^{-1}$ )
<b>Oxides</b>					
Al <sub>2</sub> O <sub>3</sub>	2054 ± 6	47.70	Mullite	1850	
BaO	2013	25.80	Na <sub>2</sub> O ( $\alpha$ )	1132	33.90
BeO	2780 ± 100	30.54	Nb <sub>2</sub> O <sub>5</sub>	1512 ± 30	58.40
Bi <sub>2</sub> O <sub>3</sub>	825		Sc <sub>2</sub> O <sub>3</sub>	2375 ± 25	
CaO	2927 ± 50		SrO	2665 ± 20	25.60
Cr <sub>2</sub> O <sub>3</sub>	2330 ± 15	49.80	Ta <sub>2</sub> O <sub>5</sub>	1875 ± 25	
Eu <sub>2</sub> O <sub>3</sub>	2175 ± 25		ThO <sub>2</sub>	3275 ± 25	
Fe <sub>2</sub> O <sub>3</sub>	Decomposes at 1735 K to Fe <sub>3</sub> O <sub>4</sub> and oxygen		TiO <sub>2</sub> (rutile)	1857 ± 20	31.50
Fe <sub>3</sub> O <sub>4</sub>	1597 ± 2	73.80	UO <sub>2</sub>	2825 ± 25	
Li <sub>2</sub> O	1570	32.00	V <sub>2</sub> O <sub>5</sub>	2067 ± 20	
Li <sub>2</sub> ZrO <sub>3</sub>	1610		Y <sub>2</sub> O <sub>3</sub>	2403	≈38.70
Ln <sub>2</sub> O <sub>3</sub>	2325 ± 25		ZnO	1975 ± 25	
MgO	2852	25.80	ZrO <sub>2</sub>	2677	29.50
<b>Halides</b>					
AgBr	434		LiBr	550	
AgCl	455		LiCl	610	22.60
CaF <sub>2</sub>	1423		LiF	848	
CsCl	645	22.17	Lil	449	
KBr	730		NaCl	800	25.90
KCl	776	25.20	NaF	997	
KF	880		RbCl	722	23.85
<b>Silicates and other glass-forming oxides</b>					
B <sub>2</sub> O <sub>3</sub>	450 ± 2	33.20	Na <sub>2</sub> Si <sub>2</sub> O <sub>5</sub>	874	31.00
CaSiO <sub>3</sub>	1544	31.00	Na <sub>2</sub> SiO <sub>3</sub>	1088	38.50
GeO <sub>2</sub>	1116		P <sub>2</sub> O <sub>5</sub>	569	
MgSiO <sub>3</sub>	1577	40.70	SiO <sub>2</sub> (high quartz)	1423 ± 50	4.6
Mg <sub>2</sub> SiO <sub>4</sub>	1898	32.76			
<b>Carbides, nitrides, borides, and silicides</b>					
B <sub>4</sub> C	2470 ± 20	38.00	ThN	2820	
HfB <sub>2</sub>	2900		TiB <sub>2</sub>	2897	
HfC	3900		TiC	3070	
HfN	3390		TiN	2947	
HfSi	2100		TiSi <sub>2</sub>	1540	
MoSi <sub>2</sub>	2030		UC	2525	
NbC	3615		UN	2830	
NbN	2204		VB <sub>2</sub>	2450	
SiC	2837		VC	2650	
Si <sub>3</sub> N <sub>4</sub>	At 2151 K partial pressure of N <sub>2</sub> over Si <sub>3</sub> N <sub>4</sub> reaches 1 atm		VN	2177	
			WC	2775	
TaB <sub>2</sub>	3150		ZrB <sub>2</sub>	3038	
TaC	3985		ZrC	3420	
TaSi <sub>2</sub>	2400		ZrN	2980 ± 50	
ThC	2625		ZrSi <sub>2</sub>	1700	

**TABLE 34.3 Predominantly Covalent Ceramics with Very High Melting Temperatures**

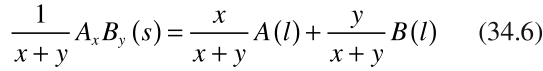
Ceramic	$T_m$ ( $^{\circ}\text{C}$ )	Covalent character of bond (%)
HfC	3890	70
TiC	3100	78
WC	2775	85
B <sub>4</sub> C	2425	94
SiC	2300	88
C (diamond)	3727	100

**TABLE 34.4 Melting Temperatures of Alkaline Earth Metal Oxides**

Oxide	$T_m$ ( $^{\circ}\text{C}$ )	Covalent character (%)	$\phi$ ( $\text{nm}^{-1}$ ) = $Z/r$
BeO	2780	37	57
MgO	2852	27	28
CaO	2927	21	20
SrO	2665	21	17
BaO	2017	18	15

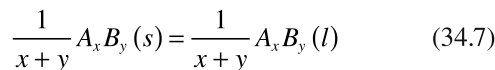
rule. Richard's rule holds fairly well for many elements (e.g., Au, Ti, Pb, Na, K, B) but not for compounds.

We can consolidate the values in Table 34.2 with Richard's rule by considering the processes involved when a compound,  $AB$ , melts. The overall melting reaction is

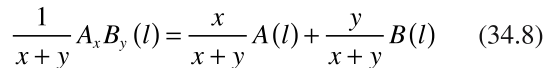


$$\Delta S_1 = \Delta S_f$$

This reaction can be broken down into two steps. First,



which gives  $\Delta S_2$  and corresponds to a hypothetical melting process in which the compound retains its ordered structure in the liquid phase. This step is followed by



which gives  $\Delta S_3 = \Delta S_m$  and represents disordering of the compound in the liquid to form a random solution. For this latter step the entropy change is given by the "entropy of mixing," which is

$$\Delta S_m = -R[X_A \ln X_A + X_B \ln X_B] \quad (34.9)$$

where  $X_A$  and  $X_B$  are the atom fractions of A and B, respectively. For our particular example we can write the entropy of mixing as

$$\Delta S_3^0 = -R \left[ \frac{x}{x+y} \ln \left( \frac{x}{x+y} \right) + \frac{y}{x+y} \ln \left( \frac{y}{x+y} \right) \right] \quad (34.10)$$

The entropies associated with each of the melting reactions given above are related as follows:

$$\Delta S_1 = \Delta S_2 + \Delta S_3 \quad (34.11)$$

We will now apply this approach to a real compound, MgO.

The entropy of fusion for MgO, given in Table 34.2, is  $\Delta S_f = 12.9 \text{ J g-atom}^{-1} \text{ K}^{-1}$ , i.e.,  $\Delta S_1 = 12.9 \text{ J g-atom}^{-1} \text{ K}^{-1}$ . The entropy of mixing,  $\Delta S_3$ , can be calculated from Eq. 34.7 as

$$\begin{aligned} \Delta S_3^0 &= -8.314 \left[ \frac{1}{2} \ln \left( \frac{1}{2} \right) + \frac{1}{2} \ln \left( \frac{1}{2} \right) \right] \\ &= -8.314 \ln \left( \frac{1}{2} \right) = 5.76 \text{ J g-atom}^{-1} \text{ K}^{-1} \quad (34.12) \end{aligned}$$

Using Eq. 34.11 this gives the entropy for the hypothetical melting reaction of  $7.14 \text{ J g-atom}^{-1} \text{ K}^{-1}$ . This value, which is closer to Richard's rule, does not consider a mixing contribution but only the vibrational change on melting such as occurs for an element. By assuming that we can apply Richard's rule as shown above then it is possible to determine  $\Delta S_1$  ( $\Delta S_f$ ), where such values are not available in the literature, and hence obtain  $\Delta H_f$ .

### 34.4 VAPORIZATION

Most ceramics have very high  $T_b$ . Consequently their vapor pressures are negligible at room temperature and become appreciable only at high temperature. Also very few ceramics vaporize without a molecular change. The result is that the vapor composition is usually not the same as that of the original liquid or solid. A practical consequence is that when we try to grow ceramic thin films by evaporation as described in Chapter 28 the film may have a stoichiometry different from that of the source. Some of the phenomena that can occur when compounds evaporate are shown in Table 34.5.

**TABLE 34.5 Possible Reactions during the Evaporation of Compounds**

Reaction type	Chemical reaction (M = metal, X = nonmetal)	Examples	Comments
Evaporation without dissociation	$MX(s \text{ or } l) \rightarrow MX(g)$	SiO, B <sub>2</sub> O <sub>3</sub> , GeO, SnO, AlN, CaF <sub>2</sub> , MgF <sub>2</sub>	Compound stoichiometry maintained in deposit
Decomposition	$MX(s) \rightarrow M(s) + (1/2)X_2(g)$ $MX(s) \rightarrow M(l) + (1/n)X_n(g)$	Ag <sub>2</sub> S, Ag <sub>2</sub> Se III-V semiconductors	Separate sources are required to deposit these compounds
Evaporation with dissociation Chalcogenides (X = S, Se, Te) Oxides	$MX(s) \rightarrow M(g) + (1/2)X_2(g)$ $MO_2(s) \rightarrow MO(g) + (1/2)O_2(g)$	CdS, CdSe, CdTe SiO <sub>2</sub> , GeO <sub>2</sub> , TiO <sub>2</sub> , SnO <sub>2</sub> , ZrO <sub>2</sub>	Deposits are metal-rich; separate sources are required to deposit these compounds Metal-rich discolored deposits; dioxides are best deposited in O <sub>2</sub> partial pressure (reactive evaporation)

**TABLE 34.6 Temperature at Which the Vapor Pressure Is  $10^{-4}$  torr ( $1.3 \times 10^{-2}$  Pa)**

Oxide	$T_m$ ( $^{\circ}\text{C}$ )	$T$ (vapor pressure = $10^{-4}$ torr)
PbO	890	550 $^{\circ}\text{C}$
TiO <sub>2</sub>	1640	$\sim 1300^{\circ}\text{C}$
ZrO <sub>2</sub>	2700	$\sim 2200^{\circ}\text{C}$

In many multicomponent oxide ceramics the vapor pressure of each component may be different. This effect is particularly noticeable in lead-containing compounds such as lead zirconium titanate (PZT), an important piezoelectric ceramic. PZT contains PbO, ZrO<sub>2</sub>, and TiO<sub>2</sub> in the form of a solid solution. PbO is significantly more volatile than the other two oxides (Table 34.6). As a result if PZT films are heated during processing then significant Pb loss can occur, leading to a change in film stoichiometry and dramatically different properties. If Pb loss is to be avoided then special precautions must be taken. For example, we can compensate for Pb loss by making our starting films Pb rich.

### 34.5 THERMAL CONDUCTIVITY

At all temperatures the atoms in a solid are vibrating about their equilibrium positions with a set of characteristic frequencies,  $\nu$ , with values as high as  $10^{12}$  Hz at room temperature. The energies of the lattice vibrations are quantized and given by

$$E = \left( n + \frac{1}{2} \right) h\nu \quad (34.13)$$

where  $n$  is an integer, which is zero at 0 K, and  $h$  is Planck's constant. At absolute zero the atoms have  $E = h\nu/2$ : the zero point energy. If the solid is heated  $E$  will increase in integer steps of  $h\nu$  and similarly if the solid is cooled the vibrational energy will decrease in steps of  $h\nu$ . You can see immediately that there is a similarity between this process and the absorption or emission of light (*photons*). And so the name *phonon* is used as the quantum unit of lattice vibrational energy.

Wave-particle duality applies equally to phonons as it does to photons. Thus, phonons possess the characteristics of both waves and particles. In ceramics the conduction of heat is primarily due to the movement of phonons. When a ceramic is heated we can think in terms of an increase in the number of phonons. When there is a temperature dif-

ference phonons move from the high temperature end, where their concentration is high, to the lower temperature end, where their concentration is lower. The driving force is the concentration gradient, just as it is in the diffusion of matter. The rate of heat flow  $dq/dt$  is proportional to the temperature gradient  $dT/dx$ , where the constant of proportionality is the thermal conductivity,  $k$ :

$$\frac{dq}{dt} = -kA \frac{dT}{dx} \quad (34.14)$$

where  $A$  is the cross-sectional area normal to the direction of heat flow.

Thermal conductivity depends on three factors:

1. Heat capacity  $C$
2. Average particle velocity,  $\nu$
3. Mean free path of a particle between collisions,  $l$

From the kinetic theory of gases the thermal conductivity of an ideal gas is

$$k = \frac{1}{3} C\nu l \quad (34.15)$$

#### $\nu$ AND $l$ FOR ELECTRONS AND PHONONS

For electrons in a metal at room temperature,  $\nu \sim 10^6$  m/s and  $l \sim 10$  nm.

For phonons in a ceramic at room temperature,  $\nu \sim 10^3$  m/s and  $l \sim 1\text{--}4$  nm.

The phonon mean free path greatly increases with decreasing temperature; it is  $\sim 10$   $\mu\text{m}$  at 20 K.

Debye (in 1914) applied Eq. 34.15 to phonon conduction to describe thermal conductivity in dielectric solids. Then  $C$  is the heat capacity of the phonons,  $\nu$  is the phonon velocity, and  $l$  is the phonon mean free path.

Phonon conduction in ceramics is very different from that found in metals where the free electrons are the source of the thermal conductivity. The mobility of phonons is usually significantly lower than that of electrons because they are scattered by lattice vibrations (i.e., other phonons). Conse-

#### VIBRATIONAL AMPLITUDES

In a solid these may be as large as 0.02–0.03 nm.

quently ceramics generally have low thermal conductivities. However, the phonon mechanism can be very effective and it is often a surprise to realize that the thermal conductivity of some ceramics is actually higher than that of metals! At temperatures above  $\sim 50$  K, diamond has the highest thermal conductivity of any known material. The thermal conductivity of a gem quality diamond is in the range of  $2000\text{--}2500 \text{ W m}^{-1} \text{ K}^{-1}$  at room temperature whereas that of copper is  $400 \text{ W m}^{-1} \text{ K}^{-1}$ . Values for the room temperature thermal conductivity of some selected ceramics are given in Table 34.7.

Ceramics having high thermal conductivities generally share the following characteristics:

**TABLE 34.7 The Thermal Conductivity of Some Ceramics**

Material	$k$ ( $Wm^{-1}K^{-1}$ )	Material	$k$ ( $Wm^{-1}K^{-1}$ )
Al <sub>2</sub> O <sub>3</sub>	30.0–35.0	Spinel (MgAl <sub>2</sub> O <sub>4</sub> )	12.0
AlN	200.0–280.0	Soda–lime–silicate glass	1.7
BeO	63.0–216.0	TiB <sub>2</sub>	40.0
MgO	37.0	PSZ	2.0
SiC	84.0–93.0	SiAlON	21.0
SiO <sub>2</sub>	1.4	Si <sub>3</sub> N <sub>4</sub>	25.0
Cordierite (Mg–aluminosilicate)	4.0	Forsterite	3.0

- Strong interatomic bonding
- Simple crystal structure
- Comprise light elements that are close together in the periodic table

From Table 34.7 you can see that BeO and AlN are examples of ceramics with high thermal conductivity and both these materials satisfy the conditions given above.

Figure 34.3 shows the thermal conductivity of single crystal alumina as a function of temperature. At very low temperatures the mean free path,  $l$ , of the phonons becomes comparable to the size of the specimen and  $k$  depends mainly on the heat capacity, which increases with  $T^3$ . The thermal conductivity reaches a maximum at some low temperature (~ 40K in this case). As the temperature increases  $k$  decreases because there are more phonons

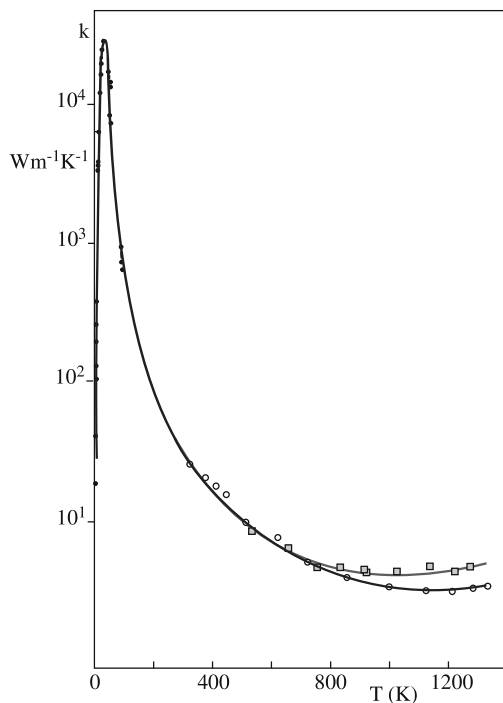


**FIGURE 34.3** Thermal conductivity of single crystal aluminum oxide over a wide temperature range. The variation in the data above 800K is due to the differences in the experimental method used.

around with which to collide and more chances of a scattering event taking place. The interactions between phonons was first described by Rudolf Peierls (1929) who identified two types of scattering processes:

- Umklapp (from the German *umklappen*, which means “flipping over”)
- Normal

The normal process has no effect on the thermal resistance. However, the umklapp process leads to an increase in thermal resistance with temperature given by

$$l \propto \frac{1}{T} \quad (34.16)$$

Eventually  $l$  decreases to a value close to the interplanar spacing and  $k$  due to phonon transport becomes temperature independent. The temperature variation of  $l$  for several ceramics is shown in Figure 34.4.

At high temperatures part of the thermal energy may also be transferred by radiation. The radiant energy conductivity,  $k_r$ , is given by

$$k_r = \frac{16}{3} \sigma n^2 T^3 l_r \quad (34.17)$$

where  $\sigma$  is the Stefan–Boltzmann constant,  $n$  is the refractive index, and  $l_r$  is the mean free path of the photons responsible for radiant heat transfer.

Some single crystals and glasses have good transparency in the visible and in frared (IR) parts of the electromagnetic spectrum and  $l_r$  can become large. In most polycrystalline ceramics,  $l_r$  is very short because of absorption and scattering, mainly due to the presence of pores. For opaque materials  $l_r \sim 0$  and radiation transfer is negligible except at very high temperatures.

At the other extreme when  $l_r$  is very large there is no interaction with the material and radiation heat transfer

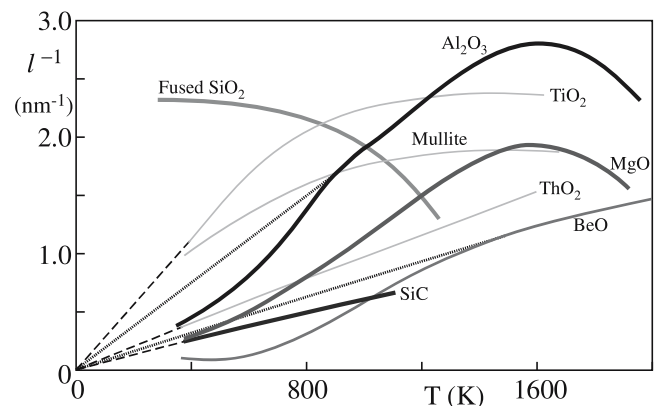


**FIGURE 34.4** Inverse phonon mean free paths for several crystalline oxides and for vitreous silica.

becomes a surface effect. The contribution of  $k_r$  to the overall thermal conductivity becomes significant only when  $l_r$  is small compared with the sample size but large compared with atomic dimensions.

In ceramics with mobile electrons or holes there is a third mechanism that can contribute to thermal conductivity. The electronic thermal conductivity  $k_e$  is

$$k_e \propto \exp\left(-\frac{E_g}{kT}\right) \quad (34.18)$$

where  $E_g$  is the band gap energy and  $k$  is Boltzmann's constant.

In most ceramics the electronic contribution to the overall thermal conductivity is negligible. However, it can be significant in electrically conducting and semiconducting ceramics such as SiC, TiC, and graphite.

### 34.6 MEASURING THERMAL CONDUCTIVITY

There are several methods available to measure  $k$ , but no single one is appropriate for all ceramics because of their wide range of thermal conductivities. The laser flash method illustrated in Figure 34.5 is one of the most popular. In this technique a laser pulse is used to rapidly heat one face of the ceramic, which is in the form of a thin plate. A typical laser would be an Nd: glass laser producing radiation with  $\lambda \sim 1060$  nm. The energy of each laser pulse is  $\sim 15$  J. An IR detector measures the temperature of the face remote from the laser. The time taken for the peak in the temperature profile to reach the remote face of the sample and the reduction in the peak temperature are measured. These measurements provide us with the thermal diffusivity,  $D_{th}$ , and the heat capacity,  $c_p$ . If the density,  $\rho$ , of the ceramic is known then  $k$  can be obtained using

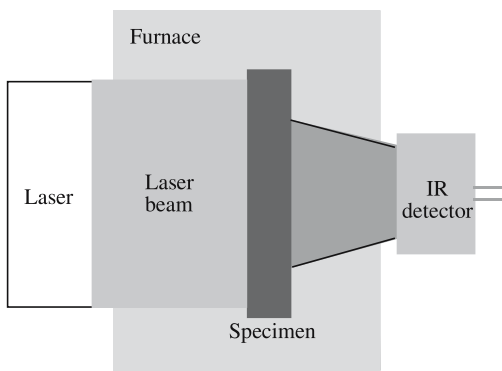


**FIGURE 34.5** Schematic of the laser flash method used for measuring thermal conductivity of ceramics.

$$k = \rho c_p D_{th} \quad (34.19)$$

The measurements can be performed at room temperature or at a range of higher temperatures by enclosing the sample in a furnace.

### 34.7 MICROSTRUCTURE AND THERMAL CONDUCTIVITY

As mentioned in Chapter 1, thermal conductivity depends on microstructure. Anything that changes the local atomic arrangement or induces elastic strains in the lattice will decrease  $l$ .

- **Impurities.** The presence of impurities disrupts the normal lattice arrangement. As temperature increases the effect of the impurity becomes less because  $l$  approaches the dimensions of the unit cell. The effect on  $k$  is illustrated for solid solutions in the isomorphous system MgO–NiO in Figure 34.6.
- **Porosity.** The thermal conductivity of air is only  $0.026 \text{ W m}^{-1} \text{ K}^{-1}$ , significantly less than most crystalline ceramics. Consequently ceramics containing a high volume fraction of porosity have

**MgO**

$l \sim 3 \text{ nm}$  at  $200^\circ\text{C}$ .  
 $l \sim 0.6 \text{ nm}$  at  $1000^\circ\text{C}$ .  
 $a_{\text{MgO}} = 0.421 \text{ nm}$ .

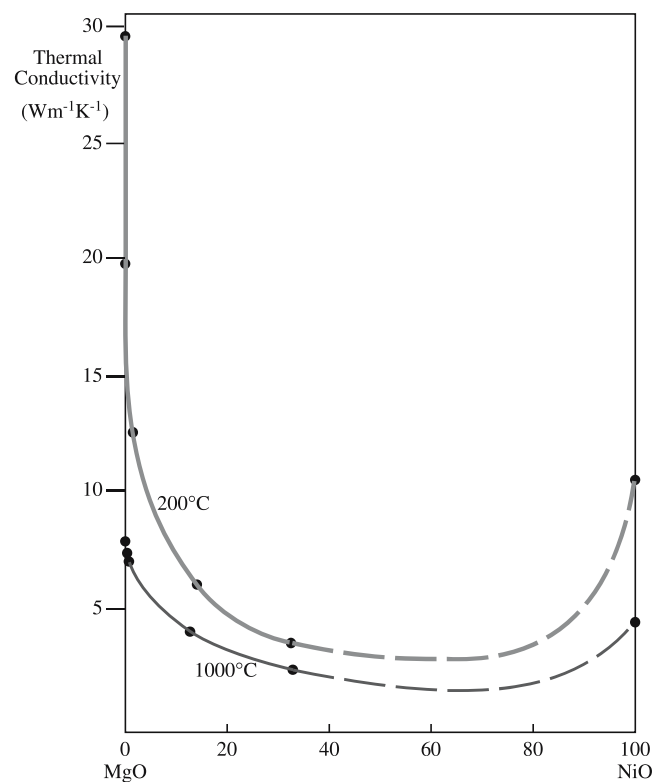


**FIGURE 34.6** The thermal conductivities of solid solutions in the MgO–NiO system.

low values of  $k$ . This property is used to good effect in designing materials for thermal insulation such as the tiles used on the outside of the space shuttle to protect it during reentry into the earth's atmosphere. The tiles consist of a porous mat of  $\text{SiO}_2$  fibers as showed earlier in Figure 15.19. The  $\text{SiO}_2$  provides the high strength and high melting temperature requirements of the tile and the porous microstructure ensures a very low  $k$ .

- **Grain size.** The mean free path of phonons at room temperature is significantly smaller than typical grain sizes in ceramics. As a result phonon scattering at grain boundaries is not important in reducing  $k$  in most practical applications. Figure 34.7 shows the temperature dependence of  $k$  for  $\text{CaF}_2$ ,  $\text{TiO}_2$ , and  $\text{Al}_2\text{O}_3$  in single crystalline and polycrystalline form. The deviation in the relative thermal conductivities at higher temperatures is due to the contribution from photon conductivity.
- **Dislocations.** A dislocation consists of a core in which the structure and density of the material is altered. Around the core there is a long-range strain field. Both these regions can cause phonon scattering. The thermal resistance associated with dislocations is proportional to the dislocation density. There is no theory that so far accounts entirely satisfactorily for the magnitude of phonon scattering by dislocations. If you want to delve into some of the theories that have been proposed much of the original work has been discussed by Nabarro (1987).

Most practical ceramics are multiphase materials in which each constituent will, in general, have a different  $k$ . The value of  $k$  for the heterogeneous material is dependent upon the amount and distribution of the different phases.

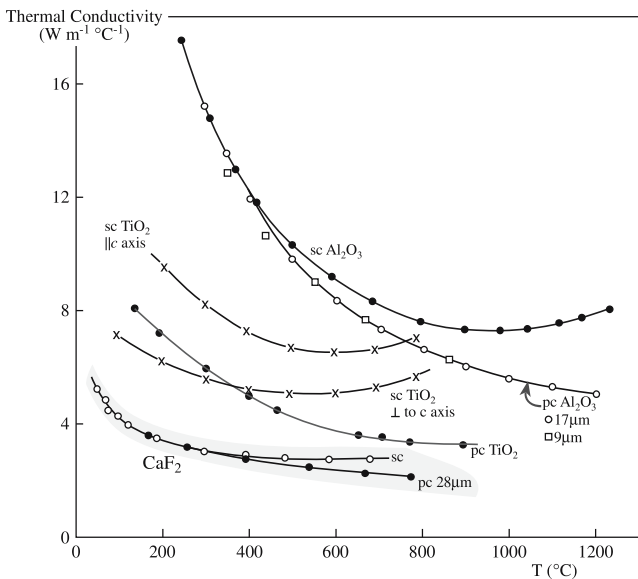


**FIGURE 34.7** Comparison of the thermal conductivity of single crystal (sc) and polycrystalline (pc) ceramics.

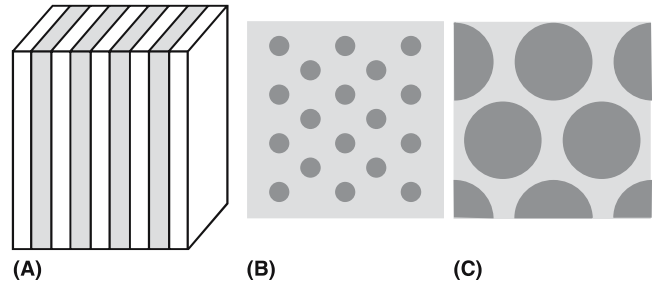


**FIGURE 34.8** Three models for the distribution of two phases in a material. (a) Parallel slabs, (b) continuous matrix phase, discontinuous particulate dispersion, and (c) large isolated grains separated by a continuous minor phase.

There are three idealized kinds of phase distributions for which equations have been derived to estimate  $k$  of the bulk material and these are illustrated in Figure 34.8 with examples summarized in Table 34.8.

- For parallel slabs with heat flow parallel to the phase boundary:

$$k_m = V_1 k_1 + V_2 k_2 \quad (34.20)$$

where  $V_1$  and  $V_2$  are the volume fractions of the two phases.

- For parallel slabs with heat flow perpendicular to the phase boundary:

$$k_m = \frac{k_1 k_2}{V_1 k_2 + V_2 k_1} \quad (34.21)$$

- For a continuous major phase:

$$k_m = k_c \left[ \frac{1 + 2V_d \left(1 - \frac{k_c}{k_d}\right) / \left(\frac{2k_c}{k_d} + 1\right)}{1 - V_d \left(1 - \frac{k_c}{k_d}\right) / \left(\frac{k_c}{k_d} + 1\right)} \right] \quad (34.22)$$

where  $k_c$  is the thermal conductivity of the continuous phase,  $k_d$  is the thermal conductivity of the dispersed phase, and  $V_d$  is the volume fraction of the dispersed phase.

TABLE 34.8 Examples of Models for Phase Distribution <sup>a</sup>		
Parallel slabs	Continuous matrix	Continuous minor
Furnace linings	Dispersed impurities	Common microstructure
Thermal barrier coatings	Common two-phase microstructure	Grain-boundary phase
Cutting tool coatings	Dispersed-particle composites	Glass-bonded ceramic
Enamels	Immiscible phases	Cermet such as Co-bonded WC
Layered composites		Reaction-sintered SiC

<sup>a</sup> See Figure 34.8.

### 34.8 USING HIGH THERMAL CONDUCTIVITY

One of the most important applications of high-*k* ceramics is as substrates and packages for electronic devices as shown in Figure 34.9. Due to the complexity and density of modern electronic devices, efficient thermal management is important. Removal of heat from the semiconductor is essential to prevent thermally induced damage.

Alumina (96 wt% Al<sub>2</sub>O<sub>3</sub>) is the most commonly used substrate material. It has a thermal conductivity in the range 15–20 W m<sup>-1</sup> K<sup>-1</sup>. The higher *k* alternatives are AlN, SiC, and BeO. Aluminum nitride is the most promising because it combines a high *k* and a high electrical resistivity (unlike SiC), it is nontoxic (unlike BeO), and it has a coefficient of thermal expansion closely matched to Si in the temperature range 25–400°C. Theoretically AlN has *k* = 320 W m<sup>-1</sup> K<sup>-1</sup>. However, in polycrystalline AlN *k* is typically in the range 50–200 W m<sup>-1</sup> K<sup>-1</sup>. One of the reasons that commercially available materials show a wide range in *k* and values lower than predicted by theory is because of the presence of impurities, mainly oxygen. When oxygen replaces nitrogen, an aluminum vacancy is formed. We can represent this process using Kröger–Vink notation (we gave the details of this notation in Chapter 11):



The aluminum vacancy leads to phonon scattering because its scattering cross section,  $\Gamma$ , for phonons is large:  $\Gamma$  is proportional to the relative difference in mass between the original site occupant and the new site occupant.

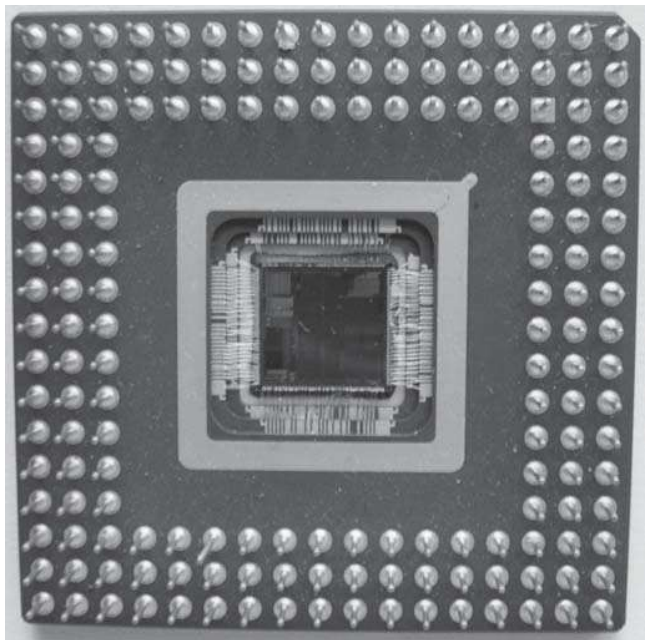


**FIGURE 34.9** A ceramic pin-grid-array package (96% pure Al<sub>2</sub>O<sub>3</sub>) with multilayer Au metallization.

$$\Gamma \propto \frac{\Delta M}{M} \quad (34.24)$$

Aluminum has an atomic weight of 27 and the vacancy has zero weight. So for our example  $\Delta M/M$  is 1. When an N atom is replaced by O on the anion sublattice  $\Delta M/M = 0.1$ . As a result the scattering cross section is smaller.

We can reduce the oxygen content in polycrystalline AlN by adding rare earth or alkaline metal oxides (such as Y<sub>2</sub>O<sub>3</sub> and CaO) to the initial powder. During sintering the additive reacts with the oxide coating on the AlN grains forming a liquid. The liquid helps in densification (as described in Section 24.7) and also acts as an oxygen “getter,” removing Al<sub>2</sub>O<sub>3</sub> from the bulk of the grains. During cooling the liquid concentrates mainly at triple points leaving mostly clean and sharp AlN–AlN grain boundaries as shown in Figure 1.4.

The record-high thermal conductivity of diamond makes it an obvious choice for consideration as a substrate for high power electronic devices. One method that has been successful in producing diamond films is chemical vapor deposition (CVD). The CVD diamond films are polycrystalline, but can still have *k* > 2000 W m<sup>-1</sup> K<sup>-1</sup>. The high cost of diamond films still precludes their widespread use.

### 34.9 THERMAL EXPANSION

We know from our everyday experiences that when we heat most materials they expand and when we cool them they contract. The linear coefficient of thermal expansion,  $\alpha$ , indicates how much the dimensions of a solid change with temperature:

$$\alpha = \frac{\Delta l}{\Delta T l_0} \quad (34.25)$$

where  $\Delta l$  is the change in length of the sample,  $l_0$  is the original length, and  $\Delta T$  is the temperature interval.

Figure 34.10 shows a typical bond–energy curve. At 0K the atoms are separated by the equilibrium spacing,  $r_0$ , which corresponds to the minimum in the bond–energy curve. The atoms will be in their lowest vibrational energy state, corresponding to the zero point energy  $h\nu/2$  and possess the minimum amplitude of vibration,  $x_0$ . When the solid is heated its energy increases as shown by the horizontal lines in Figure 34.10. The width of the trough in the bond–energy curve represents the average vibrational amplitude of the atoms for a specific energy (or  $T$ ). The average distance between the atoms is represented by the mean position along this line. A solid expands when heated because the bond–energy curve is asymmetric. If the curve was symmetric (the dashed curve in Figure 34.10) the average vibrational amplitude would increase with increasing temperature, but there would be no increase in the interatomic separation.

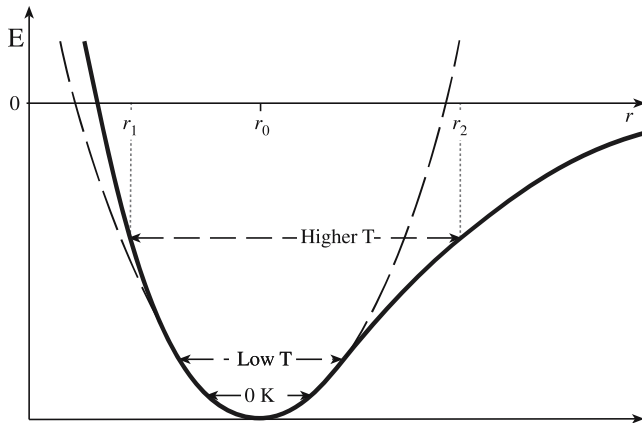


FIGURE 34.10 A typical bond-energy curve.

As described in Chapter 4 the shape of the bond-energy curve depends on the strength and type of the interatomic bonding:

- The greater the bond strength the deeper and narrower the trough in the bond-energy curve and the smaller the value of  $\alpha$ .
- The more ionic the bonding the more asymmetric the curve. Ionically bonded materials will, in general, have higher values of  $\alpha$  than covalently bonded ones.
- As melting temperature increases  $\alpha$  decreases as shown in Figure 34.11.

### AN EXAMPLE—MgO

$$\alpha = 13.5 \times 10^{-6} \text{ } ^\circ\text{C}^{-1} = 13.5 \text{ ppm}/^\circ\text{C}$$

$$\alpha (^\circ\text{C}^{-1}) \times 10^6 = 13.5; \alpha (10^6 \text{ } ^\circ\text{C})^{-1} = 13.5$$

Heating MgO from 25°C to 50°C ( $\Delta T = 25^\circ\text{C}$ ) increases  $a$  (0.421 nm at 25°C) by only 0.14 pm.

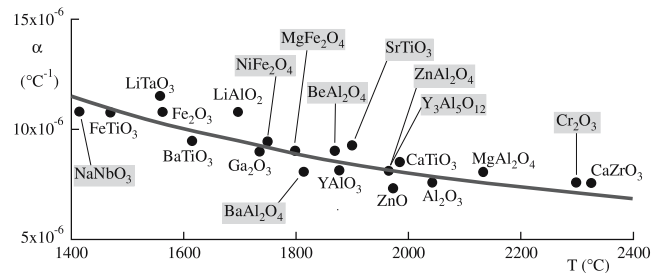


FIGURE 34.11 Plot of the average coefficient of thermal expansion versus melting temperature for many ceramics.

Values of  $\alpha$  for various ceramics are given in Table 34.9. For most ceramics  $\alpha$  lies between about  $3 \times 10^{-6}$  and  $15 \times 10^{-6} \text{ } ^\circ\text{C}^{-1}$ . Since  $\alpha$  is a function of temperature, usually increasing with increasing temperature as shown in Figure 34.12, a mean value is often quoted for a particular material over a stated temperature range.

The values in Table 34.8 are mean values and the temperature range over which these values are applicable is given. Most values of  $\alpha$  found in the literature are room temperature values and from a practical point of view it would be incorrect to use these values when considering an application over a different temperature range.

TABLE 34.9 Mean Thermal Expansion Coefficients of Various Ceramics			
Ceramic	$\alpha$ (ppm/ $^\circ\text{C}$ )	Ceramic	$\alpha$ (ppm/ $^\circ\text{C}$ )
<b>Binary oxides</b>			
$\alpha$ - $\text{Al}_2\text{O}_3$	7.2–8.8	$\text{ThO}_2$	9.2
BaO	17.8	$\text{TiO}_2$	8.5
BeO	8.5–9.0 (25–1000)	$\text{UO}_2$	10.0
$\text{Bi}_2\text{O}_3$ ( $\alpha$ )	14.0 (RT–730°C)	$\text{WO}_2$	9.3 (25–1000)
$\text{Bi}_2\text{O}_3$ ( $\delta$ )	24.0 (650–825°C)	$\text{Y}_2\text{O}_3$	8.0 ( <i>c</i> axis)
$\text{Dy}_2\text{O}_3$	8.5	ZnO	4.0 ( <i>a</i> axis)
$\text{Gd}_2\text{O}_3$	10.5	$\text{ZrO}_2$ (monoclinic)	7.0
$\text{HfO}_2$	9.4–12.5	$\text{ZrO}_2$ (tetragonal)	12.0
MgO	13.5		
<b>Mixed oxides</b>			
$\text{Al}_2\text{O}_3 \cdot \text{TiO}_2$	9.7 (average)	Cordierite	2.1
$\text{Al}_2\text{O}_3 \cdot \text{MgO}$	7.6	$\text{MgO} \cdot \text{SiO}_2$	10.8 (25–1000)
$5\text{Al}_2\text{O}_3 \cdot 3\text{Y}_2\text{O}_3$	8.0 (25–1400)	$2\text{MgO} \cdot \text{SiO}_2$	11.0 (25–1000)
$\text{BaO} \cdot \text{ZrO}_2$	8.5 (25–1000)	$\text{MgO} \cdot \text{TiO}_2$	7.9 (25–1000)
$\text{BeO} \cdot \text{Al}_2\text{O}_3$	6.2–6.7	$\text{MgO} \cdot \text{ZrO}_2$	12.0 (25–1000)
$\text{CaO} \cdot \text{HfO}_2$	3.3 (25–1000)	$2\text{SiO}_2 \cdot 3\text{Al}_2\text{O}_3$ (mullite)	5.1 (25–1000)
$\text{CaO} \cdot \text{SiO}_2$ ( $\beta$ )	5.9 (25–700)	$\text{SiO}_2 \cdot \text{ZrO}_2$ (zircon)	4.5 (25–1000)
$\text{CaO} \cdot \text{SiO}_2$ ( $\alpha$ )	11.2 (25–700)	$\text{SrO} \cdot \text{TiO}_2$	9.4 (25–1000)
$\text{CaO} \cdot \text{TiO}_2$	14.1	$\text{SrO} \cdot \text{ZrO}_2$	9.6
$\text{CaO} \cdot \text{ZrO}_2$	10.5	$\text{TiO}_2 \cdot \text{ZrO}_2$	7.9 (25–1000)
$2\text{CaO} \cdot \text{SiO}_2$ ( $\beta$ )	14.4 (25–1000)		

**TABLE 34.9** *Continued*

Ceramic	$\alpha$ (ppm/°C)	Ceramic	$\alpha$ (ppm/°C)
<b>Borides, nitrides, carbides, and silicides</b>			
AlN	5.6 (25–1000)	SiC	4.3–4.8
B <sub>4</sub> C	5.5	TaC	6.3
BN	4.4	TiB <sub>2</sub>	7.8
Cr <sub>3</sub> C <sub>2</sub>	10.3	TiC	7.7–9.5
HfB <sub>2</sub>	5.0	TiN	9.4
HfC	6.6	TiSi <sub>2</sub>	10.5
MoSi <sub>2</sub>	8.5	ZrB <sub>2</sub>	5.7–7.0
$\beta$ -Mo <sub>2</sub> C	7.8	ZrC	6.9 (25–1000)
NbC	6.6	ZrSi <sub>2</sub>	7.6 (25–2700)
Si <sub>3</sub> N <sub>4</sub>	3.1–3.7	ZrN	7.2
<b>Halides</b>			
CaF <sub>2</sub>	24.0	LiCl	12.2
LiF	9.2	LiI	16.7
LiBr	14.0	MgF <sub>2</sub>	16.0
		NaCl	11.0
<b>Glasses</b>			
Soda-lime glass	9.0	Fused silica	0.55
Pyrex	3.2		

### 34.10 EFFECT OF CRYSTAL STRUCTURE ON $\alpha$

Cubic crystals like MgO are isotropic because they have uniform thermal expansion along the three crystallographic axes. Single crystals of noncubic structures are

anisotropic and have different values of  $\alpha$  along different crystallographic directions. Some examples are given in Table 34.10. In a polycrystalline sample of an anisotropic material such as Al<sub>2</sub>O<sub>3</sub>,  $\alpha$  would be intermediate between the single crystal values for each of the different orientations.

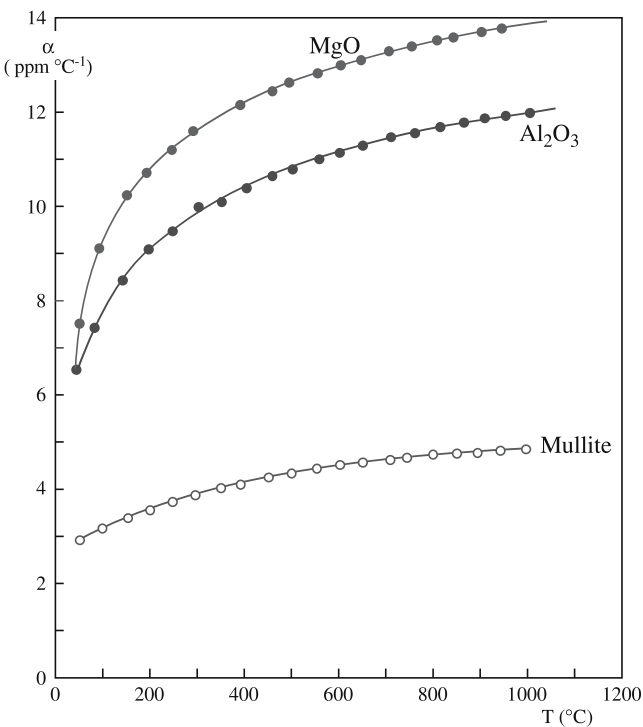


**FIGURE 34.12** Thermal expansion coefficients versus temperature for some ceramic oxides.

Some silicate minerals such as quartz (SiO<sub>2</sub>) and cordierite (Mg<sub>2</sub>Al<sub>4</sub>Si<sub>5</sub>O<sub>18</sub>) have very low coefficients of thermal expansion (for cordierite  $\alpha$  is actually negative along the *c* axis!). This property is attributed to the very open three-dimensional structure of many silicates. Cordierite is a ring silicate made up of [SiO<sub>4</sub>]<sup>4-</sup> tetrahedral units as described in Chapter 7. During heating, thermal energy can be absorbed by rearrangement of these tetrahedral units by tilting or rotating.

Structural changes that occur in a ceramic during heating can also produce a change in  $\alpha$ . An example is shown in Figure 34.13 for BaTiO<sub>3</sub>. Similar changes are

**TABLE 34.10** Thermal Expansion Coefficients for Some Anisotropic Crystals (ppm/°C)

Crystal	Normal to <i>c</i> axis	Parallel to <i>c</i> axis
Al <sub>2</sub> O <sub>3</sub>	8.3	9.0
Al <sub>2</sub> TiO <sub>5</sub>	-2.6	+11.5
3Al <sub>2</sub> O <sub>3</sub> · 2SiO <sub>2</sub>	4.5	5.7
TiO <sub>2</sub>	6.8	8.3
ZrSiO <sub>4</sub>	3.7	6.2
CaCO <sub>3</sub>	-6	25
SiO <sub>2</sub> (quartz)	14	9
NaAlSi <sub>3</sub> O <sub>8</sub> (albite)	4	13
C (graphite)	1	27

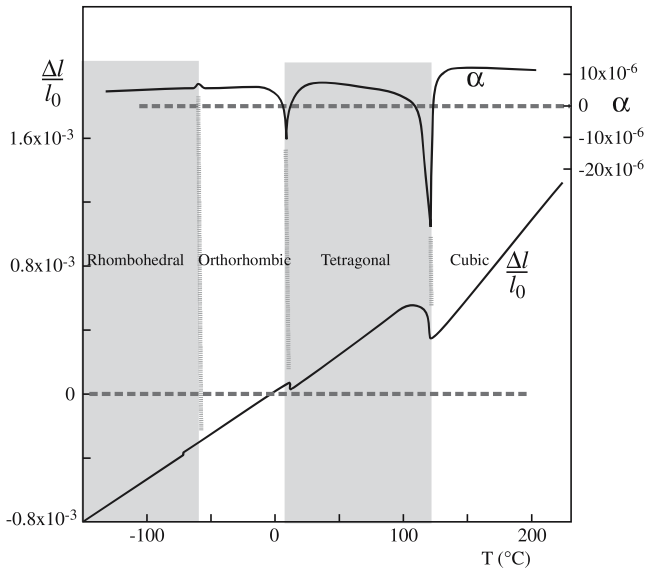


**FIGURE 34.13** The coefficient of thermal expansion of BaTiO<sub>3</sub> as a function of temperature.

seen in the crystalline forms of SiO<sub>2</sub>. Displacive phase transformations usually produce sudden changes in  $\alpha$ . Reconstructive phase changes, which involve bond breaking, usually occur more slowly and are often characterized by hysteresis.

### 34.11 THERMAL EXPANSION MEASUREMENT

The usual method of measuring  $\alpha$  is to record mechanically the change in length of a test piece as it is heated in an instrument called a push-rod dilatometer, which is illustrated in Figure 34.14. The data that are obtained are plotted as  $\Delta l/l_0$  versus  $T$  as shown in Figure 34.15. The slope of a line at any temperature is  $\alpha$ . Accuracies of commercial dilatometers can be as good as 0.5%.

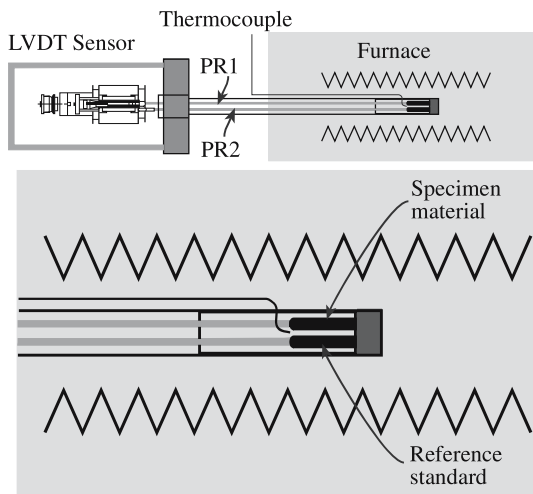


**FIGURE 34.14** Schematic of a double pushrod differential dilatometer.

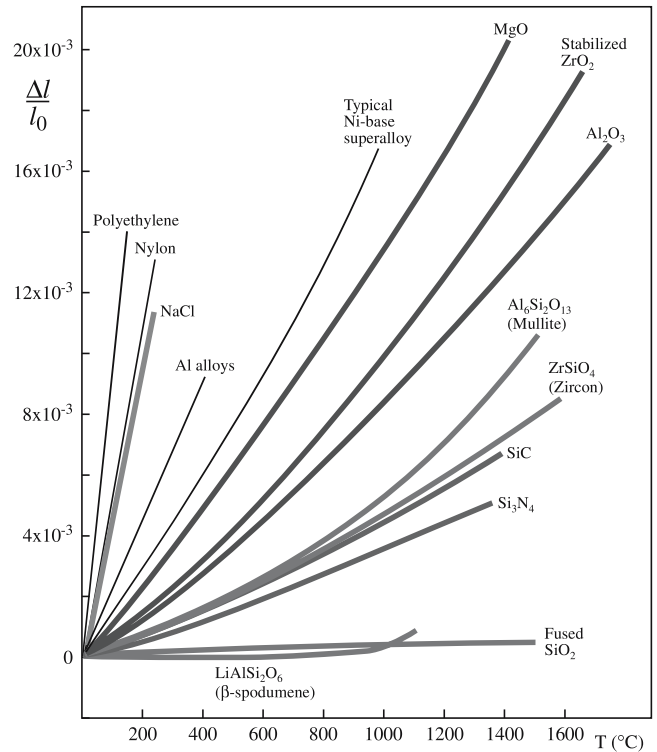


**FIGURE 34.15** Thermal expansion characteristics of several polycrystalline ceramics.

A typical plot of  $\Delta l/l_0$  versus  $T$  for a commercial silicate glass is shown in Figure 34.16. The sudden increase in  $\alpha$  in the temperature range 500–600°C is associated with the change from the glassy state into the supercooled liquid (i.e.,  $T_g$ ). The temperature range over which this change occurs depends not only on the glass composition but also on the thermal history of the glass and the rate of heating (remember  $T_g$  is not an absolute value). The decrease in length at about 700°C corresponds to the dilatometric softening temperature ( $T_d$ ), which is due to the viscous flow of the sample under the stresses imposed by

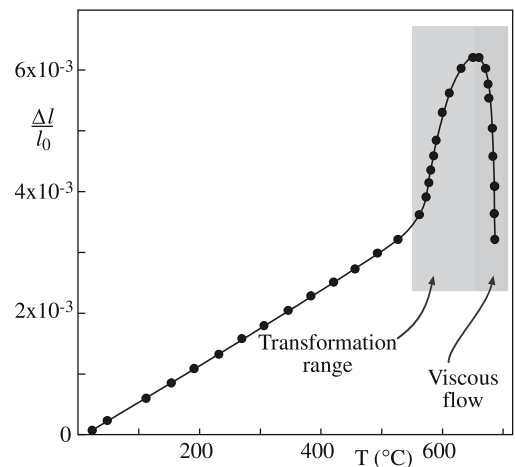


**FIGURE 34.16** Typical data for thermal expansion of a commercial silicate glass.

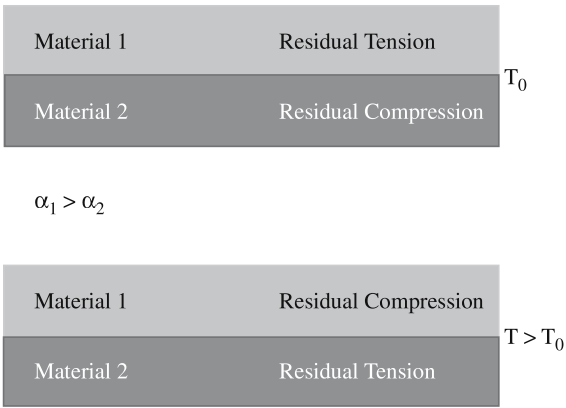


**FIGURE 34.17** Stresses generated in a layered structure due to differences in  $\alpha$ .

the dilatometer. Measurement of  $\alpha$  for a glass should always be done on well-annealed samples.

### 34.12 IMPORTANCE OF MATCHING $\alpha$ s

Thermal expansion plays a key role when two or more materials are combined in situations in which they will be subjected to changes in temperature. Consider the situation illustrated in Figure 34.17. On heating, material 1 (with the higher  $\alpha$ ) will experience a compressive stress during heating while material 2 (with the lower  $\alpha$ ) will experience tensile stresses. On cooling back down, material 1 will be in tension while material 2 will be in compression. These stresses can lead to

- Bowing
- Delamination
- Cracking

Here are some important examples:

- *Glazes on ceramics.* Most types of pottery and white-ware are coated with a glaze for both aesthetic reasons and to make the body impermeable to liquids. The glaze (like most glasses) is strong in compression yet weak in tension. Typical compressive stresses in a glaze are on the order of 70 MPa. If tensile stresses are generated they can cause cracking of the glaze as illustrated in Figure 34.18.
- *Metal to ceramic bonding.* In the packaging of semiconductor devices it is often necessary to join a ceramic (the substrate on which the “chip” is mounted) to a metal (the lead frame that provides connections to and from the outside world). The most common substrate material is a 96% wt%  $\text{Al}_2\text{O}_3$  ceramic ( $\alpha = 7.2 \times 10^{-6} \text{ }^\circ\text{C}^{-1}$ ). The Kovar metal alloys (e.g., 29%

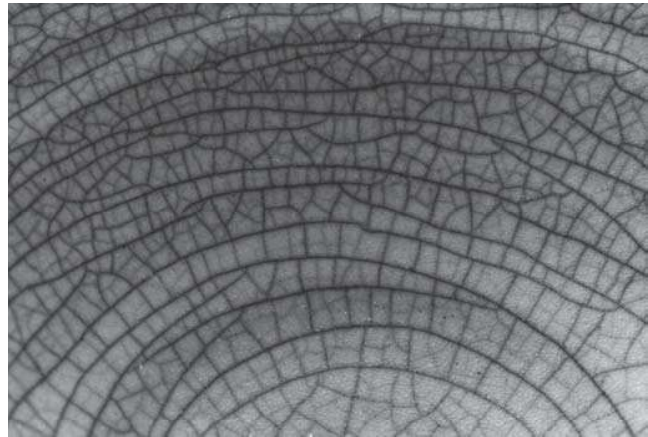


**FIGURE 34.18** Artistic cracking in a glaze as a result of stresses generated due to differences in  $\alpha$ .

Ni, 17% Co, 54% Fe;  $\alpha = 5.1 \times 10^{-6} \text{ }^\circ\text{C}^{-1}$ ) were developed to have  $\alpha$ s as close as possible to alumina.

- *Glass to metal seals.* In incandescent lamps the tungsten wire coil is fused to the glass lamp bulb to form a vacuum tight seal. The best seal is achieved when the glass and metal have similar values of  $\alpha$ . Tungsten has  $\alpha = 4.5 \times 10^{-6} \text{ }^\circ\text{C}^{-1}$ . A typical glass composition for matching with tungsten is an alkali alumina borosilicate (72.9  $\text{SiO}_2$ , 4.5  $\text{Al}_2\text{O}_3$ , 14.5  $\text{B}_2\text{O}_3$ , 3.5  $\text{Na}_2\text{O}$ , 2.4  $\text{K}_2\text{O}$ , 1.2  $\text{BaO}$ ) which has  $\alpha_{20-300^\circ\text{C}} = 4.5 \times 10^{-6} \text{ }^\circ\text{C}^{-1}$ .
- *Porcelain enameled metals.* Porcelain enameling is an established technology for bonding a coating of glass on to ferrous metal objects (e.g., stoves). The coefficient of thermal expansion of the glass must be closely matched to that of steel ( $\alpha_{1025 \text{ steel}} = 16 \times 10^{-6} \text{ }^\circ\text{C}^{-1}$ ).
- *Thin films.* Differences in  $\alpha$  between a thin film and a substrate can lead to film stress. In a thin film (where the thickness of the film is considerably less than that of the substrate), the thermal stress,  $\sigma_f$ , in the thin film is

$$\sigma_f = \frac{(\alpha_s - \alpha_f)\Delta T E_f}{(1 - \nu_f)} \quad (34.26)$$

where  $\alpha_f$  and  $\alpha_s$  are the coefficients of thermal expansion of the film and substrate, respectively,  $E_f$  is the Young’s modulus of the film, and  $\nu_f$  its Poisson ratio.

### 34.13 APPLICATIONS FOR LOW- $\alpha$

Glass-ceramics, such as the lithium-aluminosilicates (LAS), can be designed to have very low, in fact near zero,  $\alpha$ s over a wide temperature range making them particularly suitable as supports for telescope mirrors. Tele-

**EXAMPLE OF THERMAL STRESS**

Determine the thermal stress in a TiC coating deposited onto 1025 stainless steel by CVD at  $1000^\circ\text{C}$ :

$\alpha_{1025 \text{ steel}} = 16 \times 10^{-6} \text{ }^\circ\text{C}^{-1}$	$\alpha_{\text{TiC}} = 8 \times 10^{-6} \text{ }^\circ\text{C}^{-1}$
$E_{\text{TiC}} = 450 \text{ GPa}$	$\nu_{\text{TiC}} = 0.19$

Substitution into Eq. 34.26 gives  $\sigma_f = 1.67 \text{ GPa}$  at  $0^\circ\text{C}$ .

**TABLE 34.11 Comparison of Thermal Shock Parameters for a Number of Ceramics<sup>a</sup>**

Material	MOR (MPa)	$\mathcal{E}$ (GPa)	$\alpha$ (ppm/K)	$k$ ( $W\ m^{-1}\ K^{-1}$ )	$R_{TS}$ (W/m)
SiAlON	945	300	3.0	21	22,050
Hot-pressed $Si_3N_4$	890	310	3.2	15–25	13,458
Reaction-bonded $Si_3N_4$	240	220	3.2	8–12	2,727
SiC (sintered)	483	410	4.3	84	23,012
Hot-pressed $Al_2O_3$	380	400	9.0	6–8	633
Hot-pressed BeO	200	400	8.5	63	3,706
PSZ	610	200	10.6	2	575

<sup>a</sup>Poisson's ratio was taken to be 0.25 for all materials.

scopes are precise optical instruments and the resolution is very sensitive to the alignment of the mirrors and other optical components. Support materials with low  $\alpha$ s minimize thermally induced strains. A commercial glass ceramic that is used for this application is known as Zerodur<sup>TM</sup>. In addition to the very low  $\alpha$ , Zerodur is stable up to 800°C and insensitive to thermal shock. The world's largest optical mirror is located at the Parnal Observatory in the Atacama Desert in Chile. The mirror, which is made of a polished Zerodur base coated with aluminum, is 8.2m in diameter with a surface area of more than 50 m<sup>2</sup>.

### 34.14 THERMAL SHOCK

Thermal shock resistance is the ability of a material to withstand failure due to rapid changes in temperature. Ceramics and glasses are much more likely to develop thermal stress than metals because

- They generally have lower  $k$
- They are brittle

Rapid cooling of a ceramic or a glass is more likely to inflict thermal shock than heating, since the induced surface stresses are tensile. And, as you know, crack formation and propagation from surface flaws are more probable when the imposed stress is tensile.

The thermal shock resistance ( $R_{TS}$ ) of a material can be estimated using

$$R_{TS} = \sigma_f k / (\mathcal{E} \alpha) \quad (34.27)$$

where  $\sigma_f$  is the fracture stress (which for ceramics is often taken as the flexural strength or MOR) and  $\mathcal{E}$  is Young's

modulus. For high thermal shock resistance we want a ceramic with

- High  $\sigma_f$
- High  $k$
- Low  $\mathcal{E}$
- Low  $\alpha$

Values to calculate  $R_{TS}$  for several ceramics are given in Table 34.11. As an example, the  $R_{TS}$  of SiC is  $2.3 \times 10^4$  W/m, while that of  $Al_2O_3$  is 740 W/m. Ceramics such as SiC and  $Si_3N_4$ , which also have a high  $R_{TS}$ , are the most useful for components that are loaded at high temperature.

Silica glass ( $SiO_2$ ) has an  $R_{TS}$  of  $5.27 \times 10^3$  W/m. Addition of other components to the glass lowers  $\mathcal{E}$  and increases  $\alpha$ , hence decreasing  $R_{TS}$ . Soda-lime-silicate glasses such as those used for holding beverages are very susceptible to thermal shock as you have probably found out at one time or another because of their high  $\alpha = 9.2 \times 10^{-6} \text{ }^\circ\text{C}^{-1}$ . Modification of  $R_{TS}$  can most easily be accomplished by changing  $\alpha$ . The other parameters in Eq. 34.23 do not vary significantly with glass composition. If the CaO and  $Na_2O$  contents are reduced and  $B_2O_3$  is added then a borosilicate glass is formed. This is known as Pyrex<sup>TM</sup> glass ( $\alpha = 3.3 \times 10^{-6} \text{ }^\circ\text{C}^{-1}$ ), which is much more resistant to thermal shock. Most cookware and the majority of laboratory glassware are Pyrex. From a practical point of view a soda-lime-silicate glass will fail if the temperature difference is  $\geq 80^\circ\text{C}$  (so pouring boiling water into a glass beaker will certainly crack it). Pyrex glass can withstand temperature differences of 270°C before failure. Glass-ceramics with their extremely low  $\alpha$  have very high thermal shock resistance and can withstand temperature changes of  $>1000^\circ\text{C}$ .

## CHAPTER SUMMARY

The thermal properties of ceramics, like many of their other physical properties, vary over a very wide range. A good example is that of thermal conductivity. Diamond, a ceramic material, has the highest known thermal conductivity, whereas the thermal conductivity of a multiphase ceramic such as partially stabilized zirconia is three orders of magnitude lower. Thermal properties of ceramics are dominated primarily by the nature of the interatomic bonding (bond strength and ionicity). In practical ceramics we, of course, have to consider the presence of defects, impurities, and porosity as these all affect thermal properties.

## PEOPLE IN HISTORY

Debye, Petrus (Peter) Josephus Wilhelmus (1884–1966) was born in the Netherlands and became a naturalized American citizen in 1946. In 1912 he proposed the idea of quantized elastic waves, called phonons. From 1940 to 1952 Debye was Professor of Chemistry at Cornell University. He won the Nobel Prize in Chemistry in 1936.

Thomson, William (Lord Kelvin) (1824–1907), Scottish mathematician and physicist, was born in Belfast, Ireland. He proposed his absolute scale of temperature in 1848. During his life he published more than 600 papers and was elected to the Royal Society in 1851. He is buried in Westminster Abbey next to Isaac Newton.

## GENERAL REFERENCES

Berman, R. (1979) in *The Properties of Diamond*, edited by J.E. Field, Academic Press, London, p. 3. Discusses the thermal conductivity of diamond and the effect different impurities have on this property.

Kingery, W.D., Bowen, H.K., and Uhlmann, D.R. (1976) *Introduction to Ceramics*, 2nd edition, Wiley, New York, pp. 583–645. A very detailed chapter on thermal properties. The discussion of photon conductivity and the thermal properties of glasses are covered in more depth than we do.

Lynch, C.T. (1975) Ed., *CRC Handbook of Materials Science, Volume III: Nonmetallic Materials and Applications*, CRC Press, Cleveland. Relevant data for thin-film deposition are given on pp. 128–145. A useful resource for vapor pressures of various ceramics.

Rosenberg, H.M. (1988) *The Solid State*, 3rd. edition, Oxford University Press, Oxford, p. 96. Has a clear discussion of phonon scattering mechanisms.

## SPECIFIC REFERENCES

Debye, P. (1912) “The theory of specific warmth,” *Ann. Phys.* **39**, 789. An English translation of this classic paper appears in *The Collected Papers of P.J.W. Debye* (1954), Interscience, New York, p. 650.

Debye, P. (1914) *Vortäge über die Kinetische Theorie*, B.G. Teubner, Leipzig. The original source. In German.

Hultgren, R., Orr, R.L., Anderson, P.D., and Kelley, K.K. (1963) *Selected Values of Thermodynamic Properties of Metals and Alloys*, Wiley, New York. Useful lists of thermodynamics properties.

Kubaschewski, O., and Alcock, C.B. (1979) *Metallurgical Thermochemistry*, 5th edition, Elsevier, Oxford. More thermodynamic properties.

Nabarro, F.R.N. (1987) *Theory of Crystal Dislocations*, Dover, New York, p. 746. The Dover edition is essentially a republication of the work first published by the Clarendon Press, Oxford in 1967.

Peierls, R. (1929) “The kinetic theory of thermal conduction in crystals,” *Ann. Phys.* **3**, 1055.

## EXERCISES

- 34.1 Show that Eq. 34.4 gives energy in units of J.
- 34.2 The melting temperature of MgO is 3073 K while that of NaCl is 1074 K. Explain the reason for this difference.
- 34.3 Consider the structure of graphite. Would you expect the thermal conductivity to be the same parallel to the basal plane and perpendicular to the basal plane? If not, why not?
- 34.4 (a) Would you expect the thermal conductivity of crystalline quartz to be higher or lower than that of fused quartz? (b) Would you expect the differences in  $k$  to increase or decrease with increasing temperature? Explain the reasoning behind your answers.
- 34.5 Using the criteria given in Section 34.5 rank the following ceramics in order of increasing thermal conductivity: B<sub>4</sub>C, UO<sub>2</sub>, TiO<sub>2</sub>, and Si<sub>3</sub>N<sub>4</sub>. Explain the reasoning for your ranking.
- 34.6 Why is thermal transfer by radiation important only at high temperatures?
- 34.7 An AlN ceramic substrate contains 0.05 vol% porosity. Calculate the thermal conductivity of the ceramic at room temperature.
- 34.8 Which has the greater effect on the thermal conductivity of an AlN ceramic, 0.05 vol% porosity or 0.5 vol% of an Y<sub>3</sub>Al<sub>5</sub>O<sub>12</sub> second phase?
- 34.9 Would hot pressing or reaction bonding be the best method to produce Si<sub>3</sub>N<sub>4</sub> components for applications in which sudden changes in temperature will occur? Explain how you arrived at your answer.
- 34.10 Would the alkali alumina borosilicate glass given in Section 34.12 be a good choice to glaze a mullite crucible? If not, would you be better off using a soda-lime-silicate glaze or a pure silica glaze?